Liquid Crystals
Publication details, including instructions for authors and subscription information:
http://www.informaworld.com/smpp/title~content=t713926090

The dielectric relaxation processes in an antiferroelectric liquid crystal under cylindrical confinement

Stanisław A. Różański †[a]; Jan Thoen[a]
[a] Laboratorium voor Akoestiek en Thermische Fysica, Departement Natuurkunde en Sterrenkunde, Katholieke Universiteit Leuven, B-3001 Leuven, Belgium

To cite this Article Różański †, Stanisław A. and Thoen, Jan(2008) 'The dielectric relaxation processes in an antiferroelectric liquid crystal under cylindrical confinement', Liquid Crystals, 35: 2, 195 — 204
To link to this Article: DOI: 10.1080/02678290701813192
URL: http://dx.doi.org/10.1080/02678290701813192

Liquid Crystals,
Vol. 35, No. 2, February 2008, 195–204

Taylor & Francis
Taylor & Francis Group

The dielectric relaxation processes in an antiferroelectric liquid crystal under cylindrical confinement

Stanisław A. Różański† and Jan Thoen*

Laboratorium voor Akoestiek en Thermische Fysica, Departement Natuurkunde en Sterrenkunde, Katholieke Universiteit Leuven, Celestijnenlaan 200D, B-3001 Leuven, Belgium

(Received 17 October 2007; final form 16 November 2007)

In the cylindrical pore geometry of inorganic Anopore membranes the collective relaxation processes observed in a bulk antiferroelectric liquid crystal change considerably under confinement. The frequency degeneration of the soft and Goldstone modes present at the smectic A* (SmA*)–chiral smectic C (SmC*) phase transition in the bulk phase is removed under geometrical restrictions. The relaxation rate of the soft mode is strongly modified due to the deformation of the smectic layers in the curved geometry of the pores and is superimposed by the molecular relaxation process in the SmA* and SmC* phases. The soft mode in confinement splits into two relaxation processes, which are present through all other mesophases (SmC* and SmC^*_a). One of them is nearly temperature independent and slightly decreases in frequency in the SmC^*_a phase. This Goldstone-like process can be assigned to the highly deformed helical structure fluctuations. The second one exhibits the characteristic features for the molecular and soft mode relaxation processes depending on the temperature range. The biquadratic and the piezoelectric coupling between the tilt angle and spontaneous polarization are revealed in their temperature dependence.

Keywords: antiferroelectric liquid crystal; dielectric relaxation; cylindrical confinement

1. Introduction

The influence of different confinements on the thermodynamic, dielectric and other physical properties of ferroelectric (FLC) and antiferroelectric (AFLC) liquid crystals has resulted in growing interest due to the diversity of new intriguing phenomena observed under geometrical restrictions. Experiments have been performed with FLCs embedded in porous Anopore (*1–11*), porous Synpor membranes (*6–9*), porous glasses (*12–14*), aerogels (*15*) or dispersed with solid aerosil particles (*16–22*) and with AFLCs in Anopore (*23, 24*). The porous materials differ considerably in the topology of their inner structure, from straight good oriented and well separated cylindrical pores in Anopore membranes to a very complex organisation of interconnected channels and voids in Synpor membranes, porous glasses or aerogels. Choosing a porous material with a specific structure of the pores provides good opportunities to study the influence of the surface ordering effects and quenched random disorder effects on the ordering of the liquid crystal phases. In particular, in the case of quenched random disorder the use of aerosil dispersions allows a more precise explanation of many aspects of random confinement.

Anopore membranes are very useful in investigations of the influence of surface interactions on different liquid crystal phases because of the simple and well-defined topology of the pores and high surface to volume ratio (*25*). Dielectric (*1, 5*), X-ray (*3*) and optical measurements (*10, 11, 24*) reveal a specific orientation of the FLC and AFLC phases in cylindrical pores of Anopore. Dielectric measurements deliver information about molecular and collective dynamics of the relaxation processes and allow conclusions about molecular or smectic layer orientation in confinement. Optical and X-ray data give direct proof of the existence of the helical superstructure in the cylindrical channels and the influence of confinement on the thickness of the smectic layers.

Physical parameters, such as spontaneous polarisation, tilt angle and the value of helical pitch, are essential for the characterization of the ferroelectric chiral smectic C (SmC*) phase present in both the bulk and confined FLCs and AFLCs. Recent dielectric measurements have shown that in FLCs with a low spontaneous polarisation and a helical pitch above 1 μm confined in Anopore membrane the soft and Goldstone modes are completely undetectable due to the perfect orientation of the smectic layers perpendicular both to the long axis of the pores and the direction of the measuring electric field (*1, 4, 7, 9*). From the analysis of the nonlinear temperature

†Permanent address: Higher Vocational State School in Piła, ul. Podchorążych 10, 64-920 Piła, Poland.
*Corresponding author. Email: Jan.Thoen@fys.kuleuven.be

ISSN 0267-8292 print/ISSN 1366-5855 online

DOI: 10.1080/02678290701813192
http://www.informaworld.com

dependence of the dielectric strength near the smectic A* (SmA*)–SmC* phase transition, due to the molecular process related to the rotation of the molecules around their short molecular axis, the temperature dependence of the tilt angle in the confined SmC* phase was determined (*1*). Dielectric measurements confirmed the existence of a tilted smectic phase in cylindrical pores of Anopore membranes.

In the SmC* phase of an AFLC confined in Anopore membrane instead of the Goldstone mode two other relaxation processes were observed (*23*). One was assigned to the molecular reorientation around the short axis, which can be expected with quasi-homeotropic orientation of tilted molecules in the smectic layers perpendicularly to the axis of the pores. The second process was related to the internal curved surface of the Anopore membrane. In the FLC material CB500 having a TGBA phase (*2*) the Goldstone mode was still observed in Anopore but with a characteristic relaxation frequency shifted to the higher frequency region. Another relaxation process observed in confined CB500 was also assigned to the collective movements of the molecules attached to the pore walls. X-ray and dielectric measurements revealed in an other Anopore confined FLC material a smeared temperature dependence of the layer spacing in the SmA*–SmC* phase transition region in contrast to the bulk (*3*). Additionally, increases of the soft mode relaxation frequency by a factor of 2.5 in the SmA* phase and an increase of the Goldstone mode characteristic relaxation frequency as much as 400 times in the SmC* phase were observed.

The sign of the optical activity measured in the micro-confined ferroelectric liquid crystal DOBAMBC in the cylindrical channels of Anopore membranes is reversed with respect to the bulk material (*11*). The observed changes in optical activity could be explained either by a significant pitch reduction of the adsorbed phases or a reversal of the rotary sense of the helical structure in the confinement. Moreover, the selective reflection at the blue wavelength of light was observed in a confined AFLC, which confirms the existence of the helical structure in the cylindrical pores of Anopore with the helical axis oriented parallel to the axis of the pores (*24*).

In the present study, dielectric spectroscopy was used to investigate the influence of cylindrical Anopore confinement on the relaxation processes in a newly synthesised AFLC. Also, by using electro-optical methods, the temperature dependence of the tilt angle and spontaneous polarisation was determined. The influence of the confinement on the relaxation processes near the SmA*–SmC* phase transition and in the SmC^*_a phase is discussed taking into account the surface ordering effects in the cylindrical geometry of the pores.

2. Experimental

The liquid crystal (*S*)-(+)-4′-(1-methylheptyloxycarbonyl)biphenyl-4-yl 4-(6- heptanoyloxyhex-1-oxy)-benzoate belongs to the newly synthesised homologous series of the three-ring antiferroelectric esters (*26, 27*). This compound, besides isotropic (I), paraelectric SmA* and ferroelectric SmC* phases also has an antiferroelectric SmC^*_a phase, which can be supercooled down to about 311 K. The sequence of the phase transition temperatures is (*27*): Cr ($\leftarrow$311 K) 323.7 K $\rightarrow$ SmC^*_a $\leftarrow$ 333.5 K $\rightarrow$ SmC* $\leftarrow$ 344.9 K $\rightarrow$ SmA* $\leftarrow$ 355.2 K $\rightarrow$ I. X-ray measurements of the temperature dependence of the smectic layer spacing for this compound have shown that the ratio d(SmC*)/d(SmA*) attains in the SmC* phase a value of about 0.905 (*26, 27*), which is equivalent to a tilt angle θ of about 25.2°.

Spontaneous polarization and tilt angle measurements were performed in two different thicknesses of ITO electro-optical cells. Cells with 5 μm thickness and $12.7 \times 12.7\,mm^2$ pixel area were assembled with two glass plates covered by a semitransparent conducting layer of ITO and covered by rubbed polyimide to induce homogeneous orientation of the liquid crystal that was supplied by Awat Sp. z o.o. (Warsaw, Poland). The ITO cells with a thickness of about 1.3 μm and TM $12 \times 12\,mm^2$ pixel area have only one surface covered by rubbed polyimide. In the thinner cells the surface-stabilized ferroelectric and antiferroelectric conditions can be achieved where the helical superstructure is suppressed. The cells were filled on a gradient hot plate with the liquid crystal in the isotropic phase by capillary forces. The different textures as well as the quality of the homogeneous or homeotropic alignment of the liquid crystal in cells, mounted in an INSTEC (USA) hot stage, were observed and inspected under a Leica polarising microscope. The temperature stabilization was about ± 0.1 K.

The temperature dependence of the spontaneous polarisation was obtained by measuring the polarisation reversal current, I_P, induced by applying to the cell with the liquid crystal a triangular wave form signal (f=20 Hz, V_{pp}=30 V) created by a Hameg function generator and amplified by a FLC 2010. The current was determined by measuring the voltage drop over a R=300 kΩ resistor in series with the LC cell and stored in a HP oscilloscope. The spontaneous

polarisation was calculated from the equation:

$$P_s = \frac{1}{2S}\int_{t_1}^{t_2} I_P dt, \quad (1)$$

where S is the electrode area.

The temperature dependence of the tilt angle θ was determined from the two angular readings of the successive positions of the extinction related to the switching of the optical axis on the cone (2θ – cone angle) observed under a polarising microscope equipped with a turn table. The sample was switched using a low frequency square wave signal (f=0.1 Hz, V_{pp}=30 V) to avoid possible effects in dc voltage related to chemical decomposition of the sample by ionic currents.

The influence of the geometrical restrictions on the relaxation processes in the AFLC was probed in porous Anopore membranes (Whatman) with well defined, straight and separated cylindrical pores of diameter 200 nm and thickness about 60 µm. The membranes were cut to the proper shapes and heated several hours in a vacuum oven at a temperature of 473 K to remove water and other impurities. Next, the membranes were embedded with the AFLC in the isotropic phase and kept in these conditions several hours to ensure a complete fill. Finally, the outer surfaces of the membranes were carefully cleaned with filter paper to remove excess liquid crystal. Composite samples prepared in this way were mounted between the gold-plated electrodes of the measuring capacitor.

The complex dielectric permittivity $\varepsilon^*(\omega, T)$ was measured in the frequency range from 10^{-1} Hz to 10^7 Hz using a Novocontrol broadband dielectric spectrometer with a high resolution dielectric/impedance analyser Alpha and an active sample cell. Measurements were also performed in the bulk AFLC aligned homogeneously in the measuring capacitor with gold plated electrodes separated by 50 µm glass fibres. To obtain better orientation of the bulk AFLC the samples were slowly cooling from the isotropic to the SmA* phase. The experimental data were evaluated using superposition of Havriliak and Negami functions (*28*) and a conductivity contribution of the form:

$$\varepsilon^*(\omega,T) = \varepsilon_\infty + \sum_k \frac{\Delta\varepsilon_k}{\left[1+(i\omega\tau_k)^{1-\alpha_k}\right]^{\gamma_k}} - i\frac{\sigma_0}{2\pi\varepsilon_0 f^n}, \quad (2)$$

where τ_k is the relaxation time and $\Delta\varepsilon_k$ the relaxation strength of the k-th absorption process. The exponents α_k and γ_k describe broadening and asymmetry of the relaxation time distribution, respectively. ε_∞ is the high frequency limit of the permittivity and ε_0 is the permittivity of free space. The conductivity part, expressed by the term $\frac{i\sigma_0}{2\pi\varepsilon_0 f^n}$, dominates in the low frequency range where σ_0 is the Ohmic conductivity and n a fitting parameter.

3. Results and discussion

Spontaneous polarization and tilt angle

Figure 1 shows the temperature dependence of the spontaneous polarization measured in two different electro-optical cells with thicknesses of 1.3 µm and 5 µm. In general, the magnitude of the spontaneous polarisation can depend on the degree of alignment, the thickness of the cell, the frequency of the applied electric field and the possible contamination of the AFLC sample. The P_s changes from about zero at the SmA*–SmC* phase transition to about 90 nC cm^{-2} in the SmC* phase far away from the transition point. The values of P_s obtained for these two different thickness cells differ by about 15%. The best fits of the experimental data to the formula:

$$P_s = P_0(T_c - T)^\beta \quad (3)$$

for $T<T_c$ were obtained with fitting parameters P_0=33 nC cm^{-2} and β=0.36 for the 1.3 µm cell and P_0=28 nC cm^{-2} and β=0.36 for the 5 µm cell. The value of the β parameter seems to be independent on the cell thickness. This value of the critical parameter β differs from the value of 0.5 theoretically predicted by a simplified mean field model (*29*).

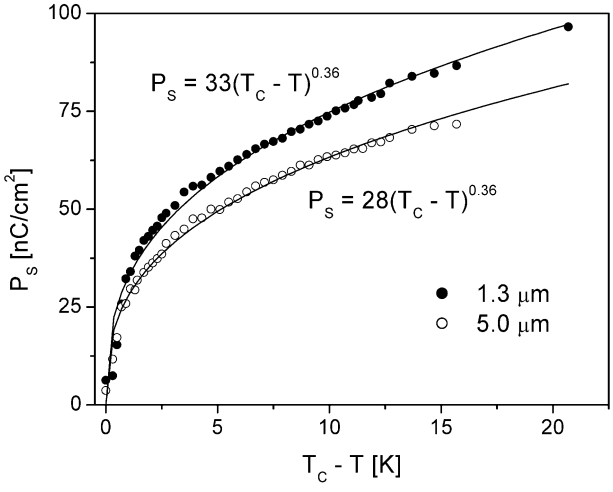

Figure 1. Temperature dependence of the spontaneous polarization, P_s, measured in electro-optical cells with different thicknesses. The solid lines represent fits to the power law of equation (3).

Figure 2 shows the temperature dependence of the tilt angle in the SmC* phase of the bulk AFLC. At the lowest temperature of the ferroelectric phase the tilt angle reaches a value of about $30 \pm 2^{\circ}$. The temperature dependence of the tilt angle can be fitted to the equation:

$$\theta = \theta_0 (T_c - T)^{\alpha}, \tag{4}$$

where θ_0 and α are fitting parameters, with α a critical exponent. The obtained fitting values of the parameters are $\theta_0 = 15^{\circ}$ and $\alpha = 0.30$. The critical exponent α also significantly differs from the value 0.5. The obtained critical parameters α and β differ considerably, which implies a nonlinear relation between the spontaneous polarization and the tilt angle (see the inset in Figure 2). This suggests the existence of a biquadratic and a piezoelectric coupling between the tilt angle and the spontaneous polarisation. Such behaviour is characteristic for ferroelectric liquid crystals with a high value of spontaneous polarisation (*30*).

Relaxation processes in cylindrical confinement

Figure 3 shows a three-dimensional plot of the temperature and frequency dependence of the dielectric losses for the homogeneously aligned AFLC in bulk and confined in the cylindrical pores of the Anopore membrane. It is immediately clear that the influence of confinement on the collective and antiferroelectric modes is remarkable.

In the isotropic phase of the bulk AFLC (Figure 3a), beside the high frequency wing of the molecular process, the conductivity contribution related with ionic free charges, present in liquid crystal, dominates. In the paraelectric SmA* phase, near the SmA*–SmC* phase transition, the soft mode (SM) (Figure 3a), related to amplitude fluctuations of the order parameter, appears. The relaxation frequency of the SM decreases with decreasing temperature but the dielectric strength increases. At the SmA*–SmC* phase transition the soft mode splits into the soft amplitude mode and the Goldstone mode (GM) related with azimuthal angle fluctuations. In the ferroelectric SmC* phase the Goldstone mode dominates and covers the much weaker soft mode. However, the SM in the SmC* phase can be extracted from the spectrum by applying during the measurements an electric field sufficiently large to unwind the helical superstructure. After crossing the

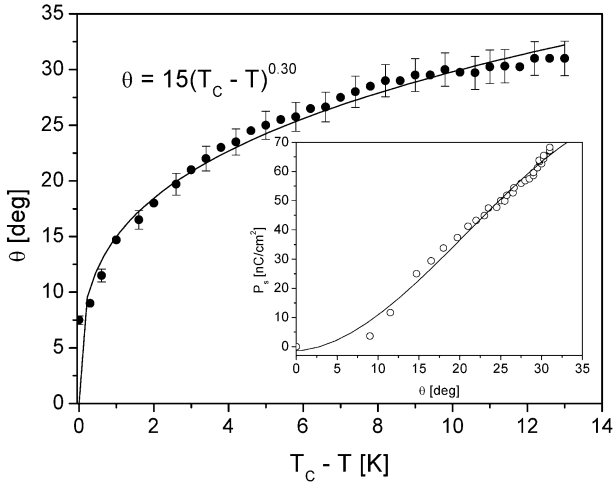

Figure 2. Temperature dependence of the tilt angle in the SmC* phase of the bulk AFLC. The solid line represents a fit to the equation (4). The inset presents the relation between the spontaneous polarisation and the tilt angle.

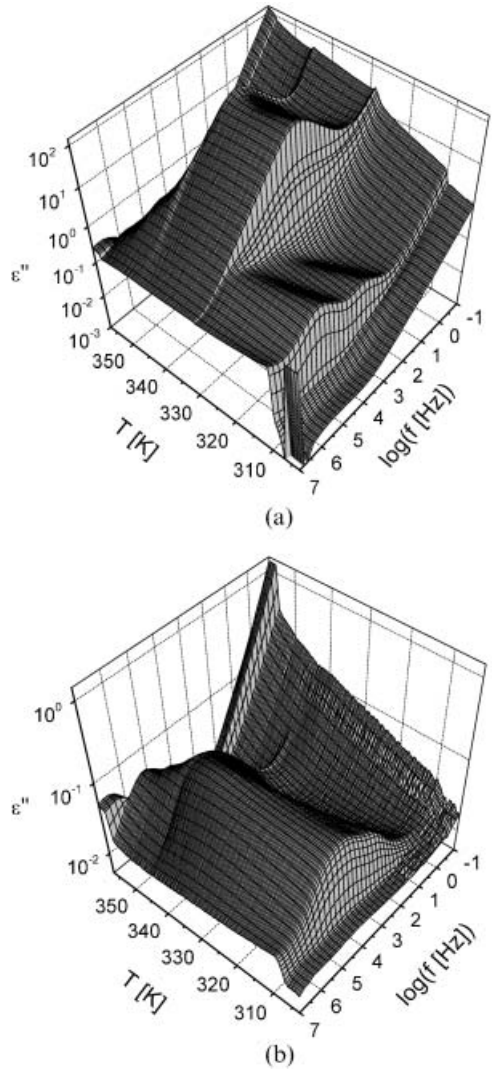

Figure 3. Temperature and frequency dependence of the dielectric losses in (homogeneously aligned) bulk AFLC (a) and AFLC confined in Anopore membrane (b).

phase transition temperature from the SmC* to the antiferroelectric SmC_a^* phase two relaxation processes appear in the dielectric spectrum, known as the high-frequency P_H and low-frequency P_L modes. A more detailed analysis of these relaxation processes has been presented previously (*31*).

In the Anopore confinement (Figure 3b) the SM is significantly modified near the SmA*–SmC* phase transition. Moreover, the Goldstone mode, dominating in the SmC* phase of the bulk AFLC, is suppressed and replaced by two relaxation processes with close relaxation frequencies that appear in all phases until crystallisation. The distinct point of the SmC*–SmC_a^* phase transition vanishes from the dielectric spectrum under confinement.

Figure 4 compares the temperature evolution of the frequency dependence of the dielectric losses in the bulk AFLC and confined in the Anopore membrane. A striking feature of the presented dielectric spectra is the considerable difference in conductivity contribution in the low-frequency range of about two orders of magnitude between the bulk AFLC and when adsorbed in Anopore. This difference results from a much lower amount of the AFLC material in the pores and also the orientation of the smectic layers hinders the conductivity in the direction parallel to the axis of the pores. In the SmA* phase the dielectric losses in confinement only slightly increase with decreasing temperature and differ in frequency dependence when compared to the bulk. After exceeding a temperature of about 345 K (Figure 4a) in the bulk very strong losses, related with the Goldstone mode in the SmC* phase, appear. However, in the Anopore membrane this process is suppressed and replaced by another process noticeably shifted to higher frequencies. At a temperature of about 329 K (Figure 4b), on approaching the SmC_a^* phase, the dielectric loss spectrum indicates the appearance of two antiferroelectric relaxation processes in the bulk AFLC. In the Anopore membrane there also appear two relaxation processes but less resolved and closer in frequency.

Figure 5 shows the frequency dependence of the dielectric losses for AFLC embedded in Anopore membrane at chosen temperatures. The solid lines represent fits to equation (2) with the fitting parameters presented in Table 1. The first, lower frequency relaxation process is characterised by decreased broadening with decreasing temperature and significant asymmetry. The second, higher

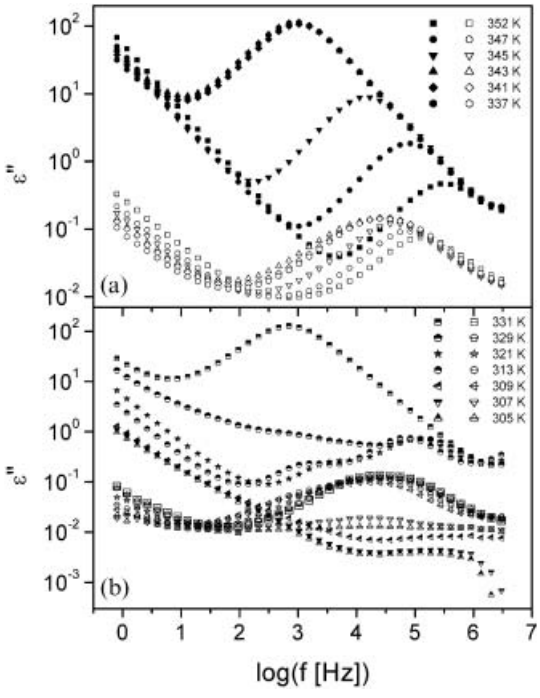

Figure 4. Comparison of the frequency dependence of the dielectric losses in the bulk AFLC (closed or half closed symbols) and adsorbed in the Anopore membrane (open symbols) at chosen temperatures. Evolution of the dielectric losses at the (a) SmA*–SmC* and (b) SmC*–SmC_a^* phase transitions.

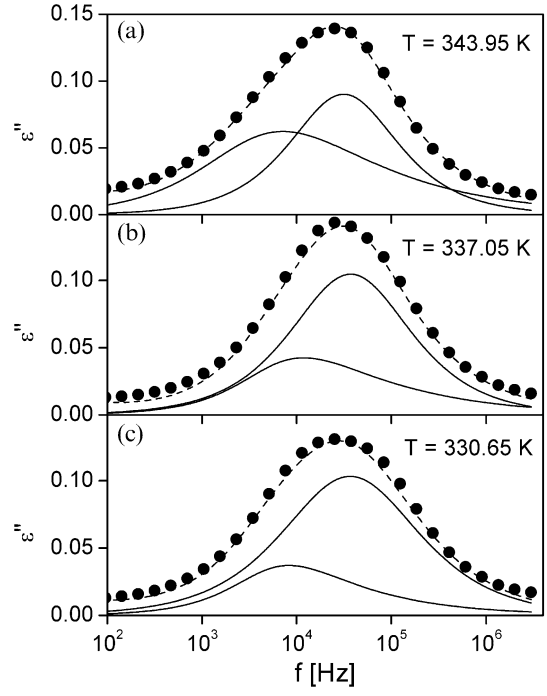

Figure 5. Frequency dependence of the dielectric losses of the AFLC confined in the Anopore membrane at chosen temperatures. The solid lines represent fits to equation (2) with fitting parameters shown in Table 1.

Table 1. Fitting parameters of the relaxation processes presented in Figure 5.

T /K	$\Delta\varepsilon_1$	τ_{1HN} /s	α_1	γ_1	$\Delta\varepsilon_2$	τ_{2HN} /s	α_2	γ_2
343.95	0.23	4.51×10^{-5}	0.22	0.53	0.21	5.07×10^{-6}	0.09	1
337.05	0.14	2.65×10^{-5}	0.05	0.46	0.27	4.24×10^{-6}	0.15	1
330.65	0.10	3.14×10^{-5}	0.02	0.55	0.30	4.32×10^{-6}	0.23	1

frequency relaxation process is described by the Cole–Cole dielectric function ($\gamma=1$) with increasing broadening with decreasing temperature.

Figure 6 shows the temperature dependence of the real part of the dielectric permittivity, $\varepsilon'(\omega, T)$, in the bulk AFLC at different frequencies. For comparison, the inset in Figure 6 shows the same frequency dependence but for the AFLC confined in Anopore membrane. In the bulk AFLC the changes of $\varepsilon'(\omega, T)$ with temperature reveal the existence of several different well-separated mesophases. The value of $\varepsilon'(\omega, T)$ characteristically increases at the SmA*–SmC* phase transition due to the appearance of the soft mode in the SmA* phase and the Goldstone mode in the SmC* phase. The value of $\varepsilon'(\omega, T)$ gradually decreases with increasing frequency in the SmC* phase as a consequence of the shift of the Goldstone mode out of the frequency window. At the higher frequencies a characteristic kink for the soft mode in the SmC* phase is visible. After passing the SmC*–SmC_a^* phase transition the values of $\varepsilon'(\omega, T)$ stay comparable to those in the isotropic phase. In the confinement the value of $\varepsilon'(\omega, T)$ is about two orders of magnitude lower than in bulk material. However, in the temperature dependence of $\varepsilon'(\omega, T)$ in confinement there is no distinction between the SmC* and SmC_a^* phases. A shift down at the crystallisation temperature is also observed.

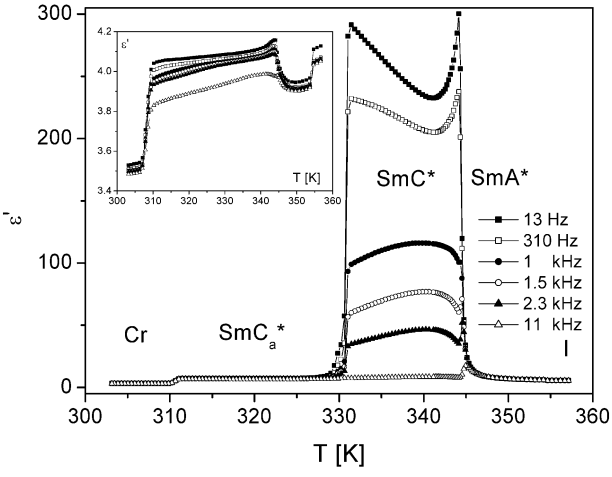

Figure 6. Temperature dependence of the real part of the dielectric permittivity $\varepsilon'(\omega, T)$ of the bulk AFLC. The inset shows the temperature dependence of $\varepsilon'(\omega, T)$ in the confined AFLC.

Figure 7 compares the temperature dependence of the relaxation rate of the processes present in the homogeneously aligned bulk AFLC and in the AFLC–Anopore composite. Beside the molecular process in the isotropic phase, in the SmA* phase of the bulk AFLC the characteristic temperature dependence of the relaxation rate for the soft mode is observed. The relaxation rate of the soft mode decreases with decreasing temperature and at the SmA*–SmC* phase transition splits into the soft amplitude mode and the Goldstone mode. The relaxation rate of the soft amplitude mode increases again with decreasing temperature but the relaxation rate of the Goldstone mode is nearly temperature independent with a typical bump near the SmA*–SmC* phase transition in the SmC* phase. The evaluation of the soft mode in the SmC* phase was described in detail previously (*31*). At the SmA*–SmC* phase transition the degeneration in the frequency of the soft mode and the Goldstone mode is observed. After passing the SmC*–SmC_a^* phase

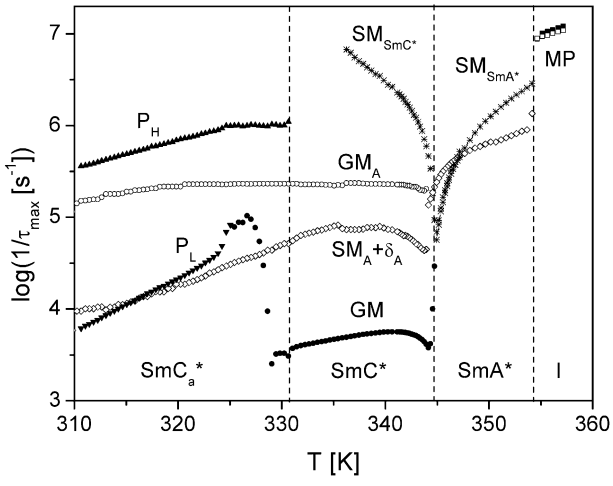

Figure 7. Temperature dependence of the relaxation rate of the relaxation processes present in the bulk AFLC (closed symbols) and confined in Anopore membrane (open symbols). Relaxation processes in the bulk AFLC: MP – molecular process in the isotropic phase; SM_{SmA^*} – soft mode in the SmA* phase; SM_{SmC^*} – soft mode in the SmC* phase; GM – Goldstone mode; P_L – low-frequency mode; P_H – high-frequency mode. Relaxation processes in the AFLC–Anopore system: MP – molecular process in the confined isotropic phase; $SM_A + \delta_A$ – superposition of the soft mode and the molecular process in confinement; GM_A – Goldstone-like mode in confinement.

transition two additional relaxation processes appear, the high-frequency P_H process and low-frequency P_L process in the antiferroelectric phase (*31–34*). The investigated AFLC is characterised by a rather high spontaneous polarisation (see figure 1) and belongs to a group of AFLC compounds with short helical pitch (*35, 36*).

In the SmA* phase of the confined AFLC the soft mode is still observed but with significantly changed temperature dependence of the relaxation rate. Below the I–SmA* phase transition the relaxation rate becomes smaller because in this range of temperature the molecular process related with rotation of the molecules around the short molecular axis, dominates. The existence of this relaxation process is imposed by the smectic layers orientation in cylindrical pores because in this geometry the measuring electric field is parallel both to the long axis of the molecule and normal to the smectic layer. However, closer to the SmA*–SmC* phase transition the characteristic dependence for the soft mode appears and is shifted in temperature by about one degree downwards compared to the bulk. The relaxation rate of the soft mode in the SmA*–SmC* phase transition is shifted to higher frequencies which indicate considerable deformation of the smectic layers in confinement. Although there is significant difference between Anopore and aerosil confinement comparable behavior was observed in FLCs dispersed with hydrophilic aerosil particles (*17–22*). This deformation and rearrangement of the smectic layers in cylindrical pores is mainly responsible for the appearance of the soft mode relaxation process in the dielectric spectrum. From the formula $\Delta T_{AC} \approx T_{AC}\left(\frac{q}{q_A}-1\right)$ (*22*) the smectic layer mismatch q/q_A can be calculated if the shift in transition temperature ΔT_{AC} and the SmA*–SmC* phase transition temperature T_{AC} is known. For $T_{AC}=345\,K$ and $\Delta T_{AC}<1\,K$ the estimated layer mismatch is rather small and equal to about 1.003. Additionally, the observed shift in the relaxation rate of the soft mode, Δf_s, at the SmA*–SmC* phase transition can be estimated from the relation $\Delta f_s \approx \frac{a_0 \Delta T_{AC}}{2\pi\gamma}$ (*22*) with typical value of material constants $a_0 \approx 5\times10^4\,N\,m^{-2}\,K^{-1}$ (*37*) and $\gamma \approx 0.1\,N\,s\,m^{-2}$. For $\Delta T_{AC}<1\,K$, the shift $\Delta f_s \approx 10^5\,Hz$ compares well with the observed gap between the soft mode frequency in confinement and the Goldstone mode frequency in the bulk AFLC.

After crossing the SmA*–SmC* phase transition the soft mode splits into the two relaxation processes that appear in the SmC* and SmC_a^* phases. A characteristic and curious feature is the disappearance of a sign of the SmC*–SmC_a^* transition point. The higher frequency process is nearly temperature independent in the measured temperature range and differs in relaxation rate less than two decades with the Goldstone mode. The origin of this relaxation process in confinement in the frequency region of about 10^5 Hz needs interpretation. First, consider the following scenario: a tilted director arrangement in the SmC* phase in the pore centre in connection with a horizontal layer configuration and an axial anchoring at the cavity walls generates a deformed director field with splayed and twisted regions at the pore walls (*5*). In the splayed area near the walls a flexoelectric polarization with a large axial component can be created which couples with the measuring electric field and contributes to the relaxation spectrum. Assuming the thickness of the splayed layer $d \sim 10\,nm$ and taking into account a typical elastic constant $K \sim 5\times10^{-12}\,N$ (*37*) and viscosity $\gamma \sim 0.1\,N\,s\,m^{-2}$ as material parameters, the estimated relaxation frequency from the formula $f=\frac{4\pi^2 K}{d^2\gamma}$ is about 10^7 Hz. The estimated value of the relaxation frequency is about two decades higher than observed in this experiment. This rather significant difference in frequencies probably excludes the above discussed mechanism as responsible for the observed relaxation process. In the second scenario, for the explanation of the origin of the observed relaxation process, one can take into account a significant deformation and rearrangement of the smectic layers in the cylindrical geometry of the pores. The arrangement of the smectic layers in confinement can be a combination of tilted smectic layer areas and perfectly oriented layers perpendicular to the axis of the pores. Therefore, the observed process can reflect a rather strongly frequency-shifted phason mode as a consequence of the elastic torque due to the lateral confinement. Recently preformed X-ray measurements reveal the considerable influence of the Anopore confinement on the temperature dependence of the tilt angle in the SmA*–SmC* phase transition (*3*), which can be connected with a compression of the smectic layers. For instance in DOBAMBC, the lateral restriction to 200 nm pores can describe the experimentally observed frequency shift of almost two decades (*12*), which is of comparable order of magnitude as in this experiment.

The temperature dependence of the relaxation rate of the second process ($SM_A+\delta_A$ in Figure 7) slightly increases in frequency near the SmA*–SmC* phase transition and behaves characteristically for a soft mode, but after approaching a kind of maximum, decreases nearly linearly with decreasing temperature and resembles the characteristic behaviour for the molecular process related with rotation of the molecule around its short axis.

Figure 8 compares the temperature dependence of the dielectric strength of the relaxation processes that appeared in the bulk AFLC and when confined in Anopore membrane. Near the SmA*–SmC* phase transition the characteristic temperature dependence of the dielectric strength for the soft mode is observed (Figure 8a), which increases rapidly in the SmA* phase and decreases in the SmC* phase with decreasing temperature. In the SmC* phase the Goldstone mode dominates with a relatively high value of dielectric strength and is nearly independent of the temperature and with a characteristic bump close to the SmA*–SmC* phase transition, related to the appearance of the helical structure in the SmC* phase. In the SmC_a^* phase two antiferroelectric modes appear, one with dielectric strength that slightly increases with decreasing temperature (P_H mode) and a second one with dielectric strength that somewhat decreases with decreasing temperature (P_L mode). In the Anopore confinement the temperature dependence of the dielectric strength changes significantly. The dielectric strength of the soft mode in the SmA* phase is much lower in confinement due to the smaller amount of LC material in the pores compared to the bulk sample, and because only a small part of the sample embedded in the pores is oriented in the proper direction to detect the soft mode (the measuring electric field is always directed parallel to the axis of the cylindrical channels). In the SmC* and SmC_a^* phases two relaxation processes appear with very low dielectric strengths almost temperature independent, except in the vicinity of the SmA*–SmC* phase transition where the dielectric strength nonlinearly changes with decreasing temperature.

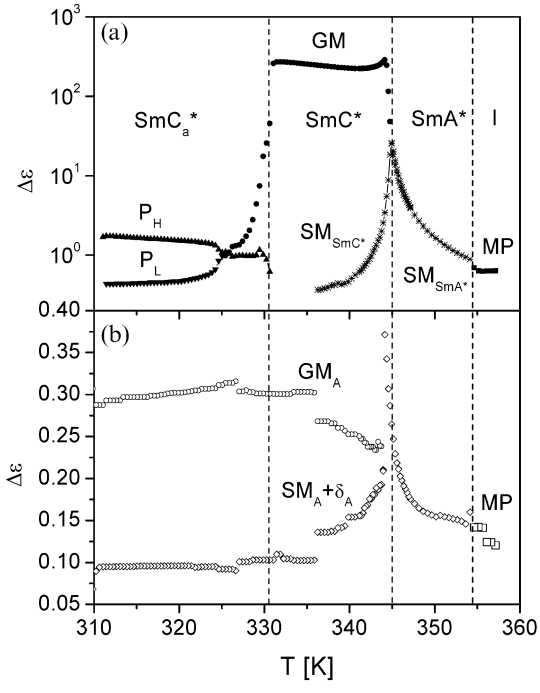

Figure 8. Temperature dependence of the dielectric strength of the relaxation processes observed in the bulk AFLC (a) and confined in Anopore membrane (b). The meaning of the labels for the different relaxation processes is identical to those for Figure 7.

It is well established in many dielectric experiments (*31–34*) that in planar geometry when the smectic layers of the bulk AFLC are perpendicular to the plates of the measuring capacitor (measuring electric field perpendicular to the helical axis) several molecular and collective relaxation processes are observed. In the paraelectric SmA* phase the soft mode then appears and splits up in the ferroelectric SmC* phase in the soft amplitude mode and the Goldstone mode. Additionally, in the antiferroelectric SmC_a^* phase two relaxation processes P_H and P_L are present. In the homeotropic geometry when the smectic layers of the bulk AFLC are parallel to the plates of the measuring capacitor (measuring electric field parallel to the helical axis) only one relaxation process related to the rotation of the molecule around its short molecular axis is observed. In this second case due to the geometry of the experiment the soft, Goldstone, P_H and P_L modes are all inactive and not dielectrically detectable.

However, in real samples the situation can be more complex and besides the soft and Goldstone modes other low-frequency relaxation processes can be observed namely domain modes (*38*) or defect mode (*39*). In thin enough planar samples the helical structure can be significantly deformed and unwound for some critical thickness. In this situation the dielectric strength and relaxation frequency are strongly thickness dependent and change with increasing geometrical restrictions (*40*).

The dielectric measurements of the present AFLC (with rather high value of spontaneous polarisation) embedded in cylindrical pores of Anopore membrane reveal significant differences with the dynamics of the relaxation processes present in the bulk. It is know from previous experiment (*1*) that for the perfect orientation of the smectic layers in the cylindrical pores (helical axis parallel to the measuring electric field) only one relaxation process related with the rotation of the molecule around short molecular axis can be detected dielectrically. Other relaxation processes as soft or Goldstone mode are then dielectrically inactive because of the experimental geometry, but not due to the influence of the geometrical restrictions. This was proved in the powdered FLC–Anopore samples (*12*).

Thus, the presence in the dielectric spectrum of the confined AFLC of several others relaxation

processes reveals that the orientation of the smectic layers is not perfect and that the structure of the smectic phases in cylindrical pores is strongly deformed and very complex. As a consequence of geometrical restrictions a significantly modified soft mode and Goldstone-like mode are now observed, with the first one superimposed with the molecular process. These relaxation processes extend into the SmC_a^* phase. However, the relatively weak P_H and P_L modes present in the bulk AFLC are missing in confinement mainly due to the geometry of the experiment although the role of the strong deformation of the SmC_a^* phase can apparently not be neglected (*41*). More decisive results regarding the structure of the present AFLC in confinement can be provided by future optical and X-ray experiments.

4. Conclusions

The dynamics of the relaxation processes present in the investigated AFLC changes considerably under Anopore confinement. The dielectric strength of the observed relaxation processes in the AFLC embedded in cylindrical pores is much reduced compared to the bulk material. The relaxation rate of the soft mode increases at the SmA*–SmC* phase transition, likely as a result of deformation and compression of the smectic layers. This mainly results from the strong competition between surface interaction and elastic forces in the curved geometry of the cylindrical pores. Moreover, as a consequence of the smectic layer deformation the SmA*–SmC* phase transition temperature T_{AC} is shifted somewhat less than one Kelvin. Additionally, in LC materials with high value of spontaneous polarisation subjected to strong surface interactions a new modulated structure can be created as a consequence of minimising the energy of the system. This can be a kind of analogy to the FLC materials subjected to the influence of a dc electric field where domain relaxation processes are observed. Two relaxation processes are observed throughout the SmC* and SmC_a^* phases without any change in frequency at the SmC*–SmC_a^* phase transition. The relaxation rate of the first process with lower relaxation frequency depends on the temperature and behaves near the SmA*–SmC* phase transition characteristically as the soft mode. This is indicated both in the temperature dependence of the dielectric strength and of relaxation frequency. However, with decreasing temperature the relaxation frequency of this soft mode also decreases, which can be the result of the superposition with the molecular process, related with rotation of the molecule around short molecular axis. The same situation appears in the SmA* phase where at higher temperatures the molecular process dominates, but close to the SmA*–SmC* phase transition the soft mode prevails. This competition between the molecular process and the soft mode in the confinement results from the distribution in orientation of the smectic layers in the cylindrical pores, which supports the existence of the molecular process and at the same time results in the appearance of the soft mode. The relaxation rate of the second process is nearly temperature independent throughout the SmC* and SmC_a^* phases and is much higher than the relaxation frequency of the Goldstone mode in the bulk SmC* phase, but lower than the relaxation frequency of the P_H process in bulk. This second process can be assigned to the phason relaxation in the strongly deformed and partially unwound helical structure in confinement.

Acknowledgements

This work has been supported by the Fund for Scientific Research Flanders, Belgium (FWO, project G.0246.02). S.A.R. acknowledges the receipt of a senior postdoctoral fellowship from the Research Council of K.U. Leuven.

References

(1) Różański S.A.; Thoen J. *Liq. Cryst.* **2006**, *33*, 1043–1049.
(2) Ray T.; Kundu S.; Roy S.K.; Roy S.S.; McLaughlin J.A.; Stannarius R. *Int. J. Mod. Phys. B* **2004**, *18*, 4119–4128.
(3) Sandhya K.L.; Krishna Prasad S.; Shankar Rao D.S.; Bahr C. *Phys. Rev. E* **2002**, *66*, 031710.
(4) Kremer F.; Huwe A.; Schönhals A.; Różański S.A., In *Broadband Dielectric Spectroscopy*; Kremer F., Schönhals A. (Eds), Springer: New York, 2002. pp. 171–224.
(5) Różański S.A.; Stannarius R.; Kremer F. *Proc. SPIE* **2001**, *4759*, 178–183.
(6) Stannarius R.; Kremer F., In *Molecules in Interaction with Surfaces and Interfaces*; Haberlandt R., Michel D., Pöppl A., Stannarius R. (Eds), Springer: New York, 2004. pp. 301–326.
(7) Różański S.A.; Stannarius R.; Kremer F. *IEEE Trans. Dielectr. Electr. Insula.* **2001**, *8*, 488–493.
(8) Różański S.A.; Stannarius R.; Kremer F.; Diele S. *Liq. Cryst.* **2001**, *28*, 1071–1083.
(9) Różański S.A.; Naji L.; Kremer F.; Stannarius R. *Mol. Cryst. liq. Cryst.* **1999**, *329*, 483–489.
(10) Binder H.; Schmiedel H.; Lantzsch G.; Cramer C.; Klose G. *Liq. Cryst.* **1996**, *21*, 415–426.
(11) Schmiedel H.; Stannarius R.; Feller G.; Cramer C. *Liq. Cryst.* **1994**, *17*, 323–332.

(12) Naji L.; Kremer F.; Stannarius R. *Liq. Cryst.* **1998**, *25*, 363–369.
(13) Aliev F.M., In *Access in Nanoporous Materials*; Pinnavaia T.J., Thorpe M.F. (Eds), Plenum Press: New York, 1995. pp. 335–354.
(14) Aliev F.M.; Kelly J. *Ferroelectrics* **1994**, *151*, 263–268.
(15) Xu H.; Vij J.K.; Rappaport A.; Clark N.A. *Phys. Rev. Lett.* **1997**, *79*, 249–252.
(16) Różański S.A.; Thoen J. *Ferroelectrics* **2006**, *344*, 63–69.
(17) Cordoyiannis G.; Nounesis G.; Bobnar V.; Kralj S.; Kutnjak Z. *Phys. Rev. Lett* **2005**, *94*, 027801.
(18) Różański S.A.; Thoen J. *Liq. Cryst.* **2005**, *32*, 331–340.
(19) Różański S.A.; Thoen J. *Liq. Cryst.* **2005**, *32*, 1013–1020.
(20) Różański S.A.; Thoen J. *J. non-crystalline Solids* **2005**, *351*, 2802–2808.
(21) Kutnjak Z.; Cordoyiannis G.; Nounesis G. *Ferroelectrics* **2003**, *294*, 105–111.
(22) Kutnjak Z.; Kralj S.; Žumer S. *Phys. Rev. E* **2002**, *66*, 041702.
(23) Ray T.; Kundu S.; Roy S.K.; Dabrowski R. *J. Mol. Liq.* **2007**, *113*, 104–110.
(24) Panarin Y.P.; Rosenblatt C.; Aliev F.M. *Phys. Rev. Lett.* **1998**, *81*, 2699–2702.
(25) Crawford G.P.; Steele L.M.; Ondris-Crawford R.; Iannacchione G.S.; Yeager C.J.; Doane J.W.; Finotello D. *J. chem. Phys.* **1992**, *96*, 7788–7796.
(26) Gąsowska J.; Dąbrowski R.; Drzewiński W.; Filipowicz M.; Przedmojski J.; Kenig K. *Ferroelectrics* **2004**, *309*, 83–93.
(27) Gąsowska J.; Dziaduszek J.; Drzewiński W.; Filipowicz M.; Dąbrowski R.; Przedmojski J.; Kenig K. *Proc. SPIE* **2004**, *5565*, 72–78.
(28) Havriliak S.; Negami S. *Polymer* **1967**, *8*, 161–210.
(29) Muševič I.; Blinc R.; Žekš B. *The Physics of Ferroelectric and Antiferroelectric Liquid Crystals*; World Scientific: Singapore, 2000.
(30) Kocot A.; Wrzalik R.; Vij J.K.; Brehmer M.; Zentel R. *Phys.Rev. B* **1994**, *50*, 16346–16356.
(31) Różański S.A.; Thoen J. *Liq. Cryst.* **2007**, *34*, 519–526.
(32) Pandey G.; Dhar R.; Agrawal V.K.; Dąbrowski R. *Phase Transitions* **2004**, *77*, 1111–1123.
(33) Pandey M.B.; Dhar R.; Agrawal V.K.; Dąbrowski R.; Tykarska M. *Liq. Cryst.* **2004**, *31*, 973–987.
(34) Buivydas M.; Gouda F.; Andersson G.; Lagerwall S.T.; Bomelburg J.; Heppke G.; Gestblom B. *Liq. Cryst.* **1997**, *23*, 723–739.
(35) Tykarska M.; Stolarz Z.; Dziaduszek J. *Ferroelectrics* **2004**, *311*, 51–57.
(36) Dąbrowski R.; Gąsowska J.; Otón J.; Piecek W.; Przedmojski J.; Tykarska M. *Displays* **2004**, *25*, 9–19.
(37) Carlsson T.; Žekš B.; Filipič C.; Levstik A. *Phys. Rev. A* **1990**, *42*, 877–889.
(38) Haase W.; Hiller S.; Pfeiffer M.; Beresnev L.A. *Ferroelectrics* **1993**, *140*, 37–42.
(39) Zubia J.; Ezcurra A.; De la Fuente M.R.; Pérez Jubindo M.A.; Sierra T.; Serrano J.L. *Liq. Cryst.* **1991**, *10*, 849–860.
(40) Novotná V.; Glogarová M.; Bubnov A.M.; Sverenyák H. *Liq. Cryst.* **1997**, *23*, 511–518.
(41) Kuczyński W.; Goc F.; Dardas D.; Dąbrowski R.; Hoffmann J.; Stryła B.; Małecki J. *Ferroelectrics* **2002**, *274*, 83–100.